

# SCIENTIFIC REPORTS



OPEN

## Light Guided *In-vivo* Activation of Innate Immune Cells with Photocaged TLR 2/6 Agonist

Keun Ah Ryu, Bethany McGonnigal, Troy Moore, Tawnya Kargupta, Rock J. Mancini & Aaron P. Esser-Kahn 

The complexity of the immune system creates challenges in exploring its importance and robustness. To date, there have been few techniques developed to manipulate individual components of the immune system in an *in vivo* environment. Here we show a light-based dendritic cell (DC) activation allowing spatial and temporal control of immune activation *in vivo*. Additionally, we show time dependent changes in RNA profiles of the draining lymph node, suggesting a change in cell profile following DC migration and indicating that the cells migrating have been activated towards antigen presentation.

Harnessing the innate and adaptive immune response has led to the development of vaccines and therapeutics<sup>1–3</sup>. However, as the immune system “rivals the nervous system in complexity<sup>4</sup>,” understanding how to design better responses and therapies remains a challenge. One area of complexity is the presentation of antigens by the innate system to the adaptive system – including chemical signaling, spatial migration and cell-cell signaling. During this process, dendritic cells (DCs), activated by Toll-like receptors (TLRs) convey pathogenic information to the cells of the adaptive immune systems through the production of cytokines and cell surface markers<sup>5, 6</sup>. This process involves the migration of activated DCs into lymphatics to present antigens to T-cells<sup>7–10</sup>. However, understanding this complex system by manipulating sets of cells within it has been a challenge. Chemical control of various innate and adaptive immune cellular processes has been a burgeoning area of interest<sup>11–16</sup>. Recently, we developed a method to tag and remotely induce a guided immune response (TRIGIR) with a photo-caged TLR2/6 agonist<sup>17</sup>. TRIGIR allows for selective labeling of cells, followed by remote light activation. Here we use the TRIGIR method for *in vivo* light-based activation to control the migration of dendritic cells. We validate our *in vivo* activation by monitoring DC migration using adoptively transferred bioluminescent DCs (Luc-DCs) that bear the TRIGIR compound.

Further, to confirm that the migrating cells were presenting antigens and further priming adaptive immune cells<sup>18, 19</sup>, we performed RNA analysis on the target lymph-node. Reported herein is a general procedure where adoptively transferred immune cells can be remotely activated using a UV light source. Though this methodology calls for a TLR2/6 bearing cell type and has limited tissue penetration of UV light used to activate the cells, it may find use in controlling activation of skin or subcutaneous DCs and for studying effects of inflammation within different spatiotemporal parameters. We expect that improvements in both optogenetic techniques, longer wavelength photo-cages, and light delivery methods will help expand the technique to answer many different immunological questions.

### Results

**Cell labeling with NPPOC-Pam<sub>2</sub>CSK<sub>4</sub>.** Previous work from our lab showed that photo-caging of the N-terminus of the TLR2/6 agonist, Pam<sub>2</sub>CSK<sub>4</sub><sup>20</sup>, can inhibit its activity to activate TLR2/6. Upon light exposure and subsequent uncaging of the N-terminus, TLR2/6 is activated by the TRIGIR compound. The intercalation of the TRIGIR compound's palmitoyl chains<sup>21</sup> on the TLR2 of DCs allows labelling of the agonists to quiescent innate immune cells without activating TLR2/6. These labelled cells can then be used in adoptive transfer experiments to achieve remote control of inflammatory processes *via* TLR2.

We sought to adapt this technique *in vivo* by labeling cells, performing subcutaneous injection and then activating of the cells in their local environment. As the agonist stays co-localized, we can have the spatial control of agonist presentation and immune cell activation<sup>17</sup>.

Department of Chemistry, University of California, Irvine, Irvine, CA, 92697, USA. Correspondence and requests for materials should be addressed to A.P.E.-K. (email: [aesserka@uci.edu](mailto:aesserka@uci.edu))

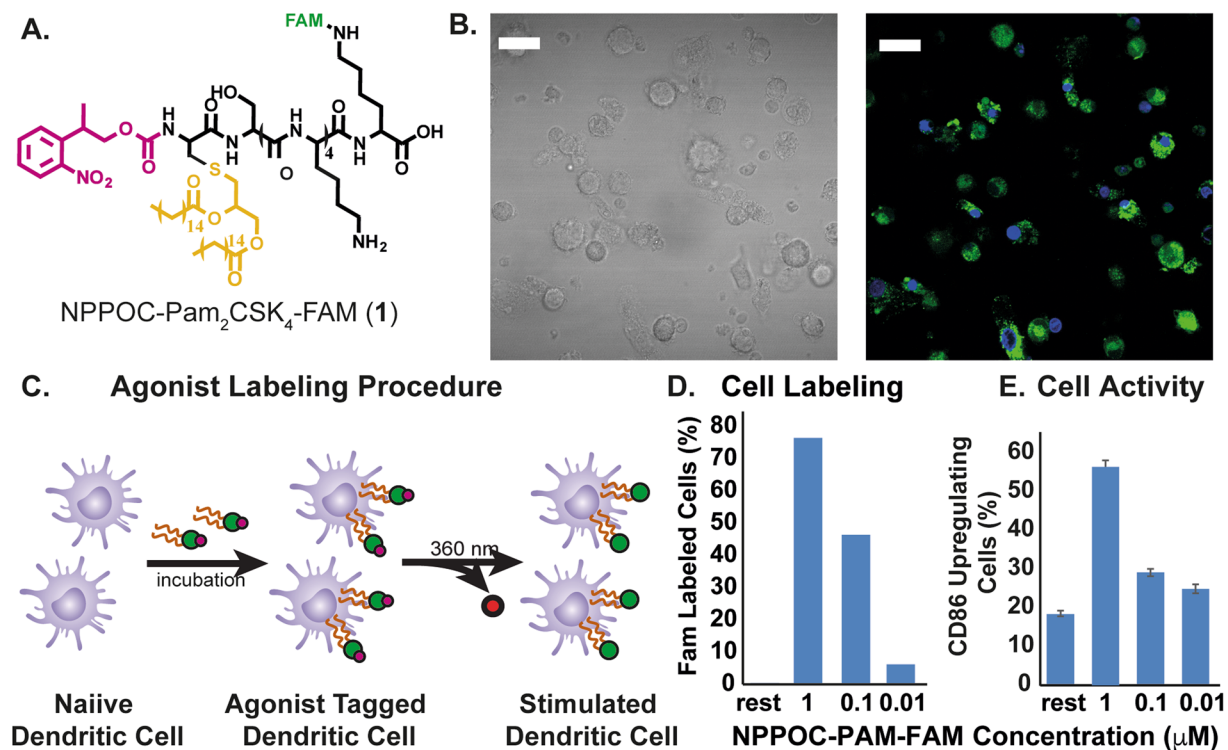


**Figure 1.** (A) Structure of photo-caged TLR 2/6 agonist NPPOC-Pam<sub>2</sub>CSK<sub>4</sub> (**1**, NPPOC-Pam-FAM) with fluorescein tag, (B) bright field and fluorescent microscopic image of labeled DCs (green-I, blue-DAPI, scale bar 10  $\mu\text{m}$ ), (C) NPPOC-Pam-FAM labeling procedure, (D) Efficiency of agonist labeling, (E) background CD86 upregulation induced by labeling DCs.

In initial experiments, we observed that high concentration of the TRIGIR compound, NPPOC-Pam<sub>2</sub>CSK<sub>4</sub> (**1**, Fig. 1A), incubation overnight resulted in higher amount of labeling of the agonist (Fig. 1D). However, this also resulted in higher background activation of the cells (Fig. 1E). Therefore, labeling the primary DCs, harvested from transgenic luciferase expressing mice, at 0.1  $\mu\text{M}$  (Fig. 1C) showed both good labeling and did not elicit a background immune response (Fig. 1D,E).

**Photo-activation of transferred dendritic cells.** Before adoptive transfer, the DCs were incubated with **1** over-night. The cells were then washed to remove excess **1** in the supernatant. The labeled cells were then injected into the footpad of mouse at 1 million cells/30  $\mu\text{L}$  for the mice. To activate the cells with light, the injected footpad of mice was then irradiated with 360 nm light (15 W) for 15 mins (Figure S1 6). To determine the limit of activity due to the limit of UV light tissue penetration, we irradiated labelled cells with 360 nm light for 15 min *in vitro* before injection. This experiment served as a “pre-activated” control and served as an upper limit for what might be achieved with photo-activated DCs *in vivo*. During the imaging process, following previously reported procedures<sup>22</sup>, we blocked the bioluminescence occurring from the injected foot with black tape to enhance the signal from the popliteal lymph node (Fig. 2).

To understand the activity of mature DCs, we compared the migration of the Pam<sub>2</sub>CSK<sub>4</sub> stimulated Luc-DCs and non-stimulated Luc-DCs that were adoptively transferred into the footpad of a mouse over a period of 96 hrs. We found the Pam<sub>2</sub>CSK<sub>4</sub> stimulated Luc-DCs migrate faster than the unstimulated Luc-DCs, where we observed migration activity as early as 24 h in Pam<sub>2</sub>CSK<sub>4</sub> stimulated Luc-DCs with a slow migration, over 96 hrs, of the unstimulated DCs into the draining lymph node at later time points (Fig. 3A,B). Because activation of dendritic cells leads to upregulation of cell surface receptors that aid in the migration and translocation of DCs into the lymph node<sup>23</sup>, we theorize that a shorter time is required for the activated cell to migrate into the lymph node compared to the unstimulated DCs.

We sought to determine if light-activation of TLR2 *via 1 in vivo* recapitulated the migration of activated DCs. We imaged the migration of the Luc-DC in mice whose footpads were exposed to UV light (+UV) or not exposed to UV (−UV). Following the trends seen in the Pam<sub>2</sub>CSK<sub>4</sub> stimulated cells, the footpads which were directly exposed to UV showed migration of Luc-DCs into the popliteal lymph node much sooner than that of the non-exposed footpads (Fig. 3A,C). Additionally, the cells that were exposed to UV migrate at a similar rate as the cells that were photo-activated before being transferred into a mouse. From this data, we conclude that TRIGIR labelled cells can be activated with light in a non-invasive manner and recapitulate the timing and quantity of their migration to the lymph node.

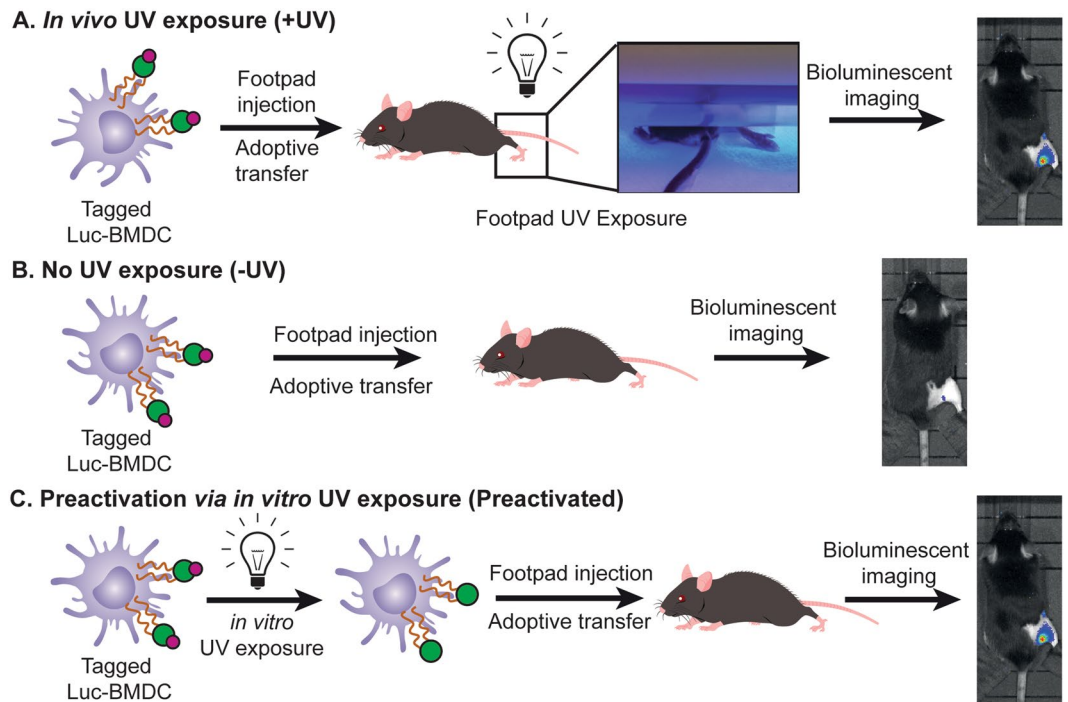


**Figure 2.** TRIGIR DC adoptive transfer procedures for (A) footpad UV irradiated mouse following adoptive transfer, (B) mouse with no UV irradiation, and (C) mouse injected with pre-irradiated tagged DCs.

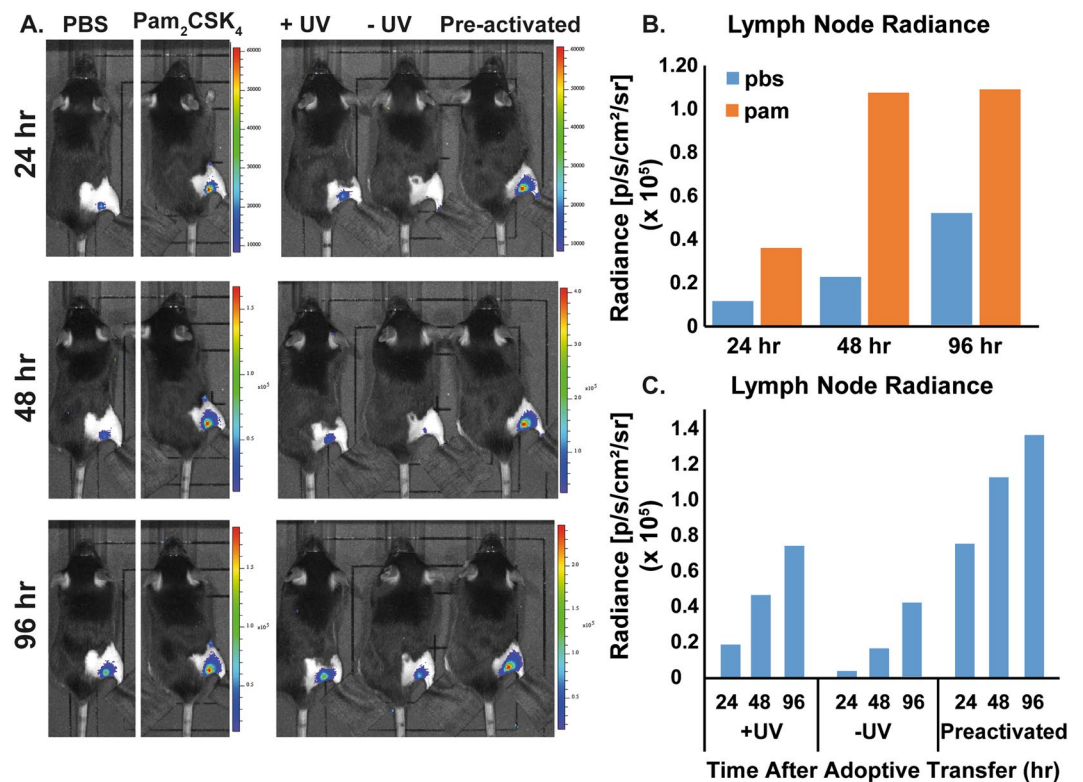


**Figure 3.** Bioluminescent image of mice taken every 24 h, over 96 h. (A) Control mice include a set of 6 mice injected with Luc-DCs preconditioned with Pam<sub>2</sub>CSK<sub>4</sub>, and a set of 6 mice injected with Luc-DCs with no preconditioning. The test set includes a set of 6 mice with TRIGIR labeled Luc-DCs followed by light exposure (+UV), one with no light exposure (-UV), and a mouse injected with TRIGIR labeled Luc-DCs exposed to light before footpad injection (pre-activated). (B) Radiance of lymph nodes of non-stimulated Luc-DCs and Pam<sub>2</sub>CSK<sub>4</sub> stimulated Luc-DCs transferred mice. (C) Radiance of lymph nodes of irradiated, non-irradiated, and pre-activated mice. Data taken from representative group.

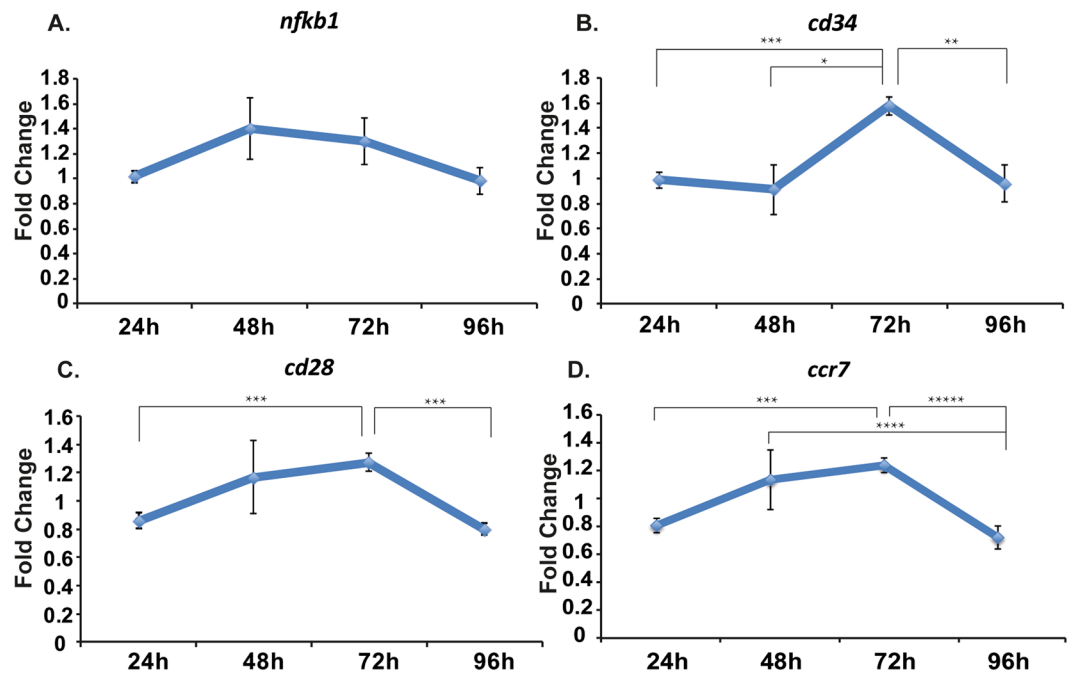


**Figure 4.** Change in gene profile in harvested lymph node of tested mice. Fold change determined by the ratio of UV irradiated and non-irradiated mice at each time point ( $n = 6$ ) of *nfkb1* (A), *cd34* (B), *cd28* (C), and *ccr7* (D). Data taken from six individual mice. \* $p < 0.0056$ , \*\* $p < 0.0028$ , \*\*\* $p < 0.0005$ , \*\*\*\* $p < 0.0008$ , \*\*\*\*\* $p < 0.035$ .

**Confirmation of systemic activation via RNA analysis of popliteal lymph node.** To further confirm the inflammatory state of TRIGIR activated DCs *in vivo* by light, we harvested popliteal lymph nodes from the mice and analyzed the RNA levels. This measurement also helped us determine if the activated DCs were enacting their antigen presenting role. If the cells were activated following light exposure, the migrated cells will elicit a systemic response as recruitment and maturation of adaptive immune cells occurs in the lymph node. We harvested lymph nodes from both light irradiated and non-irradiated animals which all contained TRIGIR-labeled DCs identical to our previous experiments. To determine differences, we plotted the changes as a relative fold-change of the from irradiated:non-irradiated at each time point. Using this measurement, we determined how irradiation and TLR stimulation changed activity in the lymph node.

First, we observed that upon TRIGIR activation, there is a gradual increase in *ccr7* which is upregulated by immune cells that enter the lymph node through recognition of CCL19 and CCL21 on the lymph node (Fig. 4D)<sup>24–26</sup>. From this we conclude there are more *ccr7* producing cells recruited into the lymph node. These cells are likely the TRIGIR activated dendritic cells which we observed migrate to the lymph node as well as T cells that have been recruited into the lymph node within the first 72 h after UV exposure as a result of DC activation.

We saw further evidence for T cell recruitment upon TRIGIR activation with an increase of *cd34* and *cd28* within the same time period. CD34 is required for T cells to enter the lymph node while blocking DC migration into the lymph node<sup>27</sup>. The downregulation of *cd34* at early time points matches the increased migration of the stimulated DCs from the footpad into the lymph node (Fig. 4B). The gradual increase suggests the increase of T cell trafficking into the lymph node and decrease in DC migration from the footpad.

Similar to the *cd34* trends, we saw a gradual increase in *cd28*, a T cell receptor that recognizes CD80 and CD86<sup>28</sup>, reaching a maximum after 72hrs (Fig. 4C). This gradual rise indicates the increase in T cell population in the popliteal lymph node. These trends follow known T cell maturation and migration following mature DC contact in the lymph node<sup>29</sup>.

In comparison, there is a general upregulation of *nfkb1*<sup>30,31</sup> starting as early as 48 hours, which could be due to the inflammatory signaling from the activated DCs that have migrated into the popliteal lymph node (Fig. 4A).

## Discussion

With our method of *in vivo* photo-activation of immune cells, we delivered a photo-caged, TRIGIR agonist and activated it in a non-invasive manner with light. Using the TRIGIR method of tagging cells, we can overcome the limitation of spatial control of soluble agonists as well as site-specific cell delivery. Compared to conventional adoptive transfer methods that require activation of cells prior to transfer to the animal our method allows for less steps in preparation of the transferred cells and controls when the cells will be activated following adoptive transfer. In addition to temporal control of cell activation, this method offers for the potential of light dosage dependent mitigation of inflammatory signals where longer irradiation times would activate more cells, allowing for sustained activation without the increasing inflammatory response.

This method can also be applied to a variety of cells to induce different responses to TLR2/6 activation. Because TRIGIR is cell specific, but requires labeling, it is compatible with many different primary cell types that can be adoptively transferred. By changing the types of cells and cell populations, one can dissect not only autocrine signaling, but also paracrine signaling following light activation of cell subsets. The technique will not limit researchers to adoptive transfer in the footpad but can create a depot of tagged, subcutaneous cells placed close to an area of interest and gain spatial and temporal control of elicited cellular response. We offer the clear caveat that current photo-activation methods will limit this method to dermal or subcutaneous activation of innate immune cells. Our data suggest that this technique will give researchers the potential to customize an innate cellular response depending on the target disease or immunological model. In conclusion, we present a method for light activation of adoptively transferred cells *via* TLR2/6. This technique presents a unique way to answer spatial and temporal questions about the innate immune response.

## Methods

All animal studies and mice maintenance were carried out in accordance with relevant guidelines and regulations approved by the Institutional Animal Care and Use Committee at University of California, Irvine (IACUC #2012-3048).

**Bone Marrow-Derived Dendritic Cell Harvest and Culture.** Bone marrow-derived dendritic cells (BMDCs) were harvested from 6-week-old B6;FVB-*Ptprca*<sup>d</sup> Tg(CAG-luc,-GFP)L2G85Chco *Thy1<sup>a</sup>/J* mice (Jackson Laboratory). Femur bones were removed from mice and the bone marrow was extracted into PBS buffer and pelleted. ACK Lysing Buffer (3 mL, Lonza) was added to the cell pellet and incubated for 2 min at RT. PBS buffer (13 mL) was then added to the cell suspension, and the cell solution was centrifuged at 300 RCF for 10 min at RT. Thereafter, the cell pellet was resuspended in BMDC complete media composed of RPMI 1640, 10% heat inactivated FBS, 20 ng/mL granulocyte-macrophage colony-stimulating factor (GM-CSF), 2 mM L-glutamine (Life Technologies), 10,000 U/mL penicillin, 10 mg/mL streptomycin, 25 µg/mL amphotericin B, and 50 µM beta-mercaptoethanol. Harvested cells were plated at  $1 \times 10^6$  cells/mL in 100 mm petri dishes (10 mL total media) and incubated at 37 °C in a CO<sub>2</sub> incubator (day 0 of cell culture). On day 3, 10 mL of fresh BMDC primary media was added to each petri dish. On day 5, BMDCs were released and plated in 24-well plates at  $5 \times 10^5$  cells/mL for cell surface marker activation, cytokine profile flow cytometry experiments.

**General Procedure for Flow Cytometry for Cell Surface Marker Upregulation.** BMDCs were incubated in individual wells with each agonist (9:1 BMDC:agonist) in 0.5 mL culture media for 18 h at 37 °C with 5% CO<sub>2</sub>. The cells were released from the plate and centrifuged at 2500 RPM at 4 °C for 10 min. The cell pellet was resuspended in cold FACS (composed of PBS (1x), 10% FBS, and 0.1% sodium azide) buffer (100 µL) and incubated with CD16/32 FcR blocking antibodies (1.0 µg/ $1 \times 10^6$  cells) on ice for 10 min. The cell suspension was pelleted and the supernatant was removed. The cell pellet was resuspended in cold FACS buffer (100 µL) and incubated with PE-CD86 (1.0 µg/ $1 \times 10^6$  cells) on ice and removed from light for 30 min. Each sample was washed twice with 300 µL cold fluorescence-activated cell sorting (FACS) buffer. The dendritic cells were resuspended in cold FACS buffer (150 µL) and kept on ice until being loaded onto the flow cytometer.

**General Procedure for Cell Labeling.** BMDCs were incubated at  $3 \times 10^6$  cells in 2 mL of media in a 6 well cell culture plate with the addition of NPPOC-Pam-FAM at 100 nM overnight at 37 °C with 5% CO<sub>2</sub>. Following incubation, the cells were collected in 15 mL conical tubes and rinsed with PBS 5 times. After the final rinse, the cells were counted and resuspended in PBS at a final cell concentration of 1 million cells/30 µL of PBS.

For the *ex vivo* UV exposed cells, the labeled cells were deprotected with 365 nm light following the last rinse, counted, and resuspended in PBS at a final cell concentration of 1 million cells/30 µL of PBS.

**General Procedure for Adoptive Transfer.** Labeled Luc-BMDCs were adoptively transferred *via* subcutaneous injection in the footpad of a C57/BL6J (Jackson Lab) mouse. The labeled cells were loaded into a syringe (10 cc, insulin syringe) at 1 million cells/30 µL of PBS. UV exposed mice were put under isofluorane (2% in 1 L/min O<sub>2</sub>) and exposed to UV light (UVP 95-01300-01 BL-15 long wave UV lamp, 15 W) for 15 mins.

**IVIS Imaging Procedure.** Luciferin was injected into each mouse (15 mg/mL in sterile PBS, 10 µL/g/mouse) *via* intraperitoneal injection. After 10 mins following the luciferin injection, the mice were anesthetized with isofluorane (2% in 1 L/min O<sub>2</sub>). Before taking images the injected foot was taped with black athletic tape and black electrical tape (3 M) to enhance the bioluminescent signal from the lymph node. Images were analyzed using Living Image Software.

**Lymph Node Tissue Harvest and RNA Extraction.** Popliteal lymph nodes were harvest following each designated time point and suspended in RNAlater solution for up to 2 weeks. The harvested RNA was homogenized with prefilled 2 mL, 1.5 mm Zirconium bead tubes at 250 G for 90 secs. The homogenized tissue solution was extracted for RNA following the procedures for RNeasy Mini Kit (Qiagen). cDNA was reverse transcribed using the extracted RNA (KIT). Murine *ccr7*, *cd34*, *cd28*, *nfb1* expression was quantified using Maxima SYBR Green/ROX qPCR Master Mix (Thermo Fisher) in the ABI 7300 detection system (Applied Biosystems). GAPDH gene expression was measured as endogenous reference. The relative fold change was calculated following the 2<sup>-ΔΔCT</sup> method<sup>32</sup>. Fold change was normalized to the average of non-irradiated mice (non treated group) and UV mice (treated group) of triplicate of 6 different mice in each group.

## References

1. Querec, T. *et al.* Yellow fever vaccine YF-17D activates multiple dendritic cell subsets via TLR2, 7, 8, and 9 to stimulate polyvalent immunity. *J. Exp. Med.* **203**, 413–424 (2006).
2. Schreiber, G. *et al.* Toll-like receptor expression and function in human dendritic cell subsets: implications for dendritic cell-based anti-cancer immunotherapy. *Cancer Immunol. Immunother.* **59**, 1573–1582 (2010).
3. Melero, I. *et al.* Evolving synergistic combinations of targeted immunotherapies to combat cancer. *Nat. Rev. Cancer* **15**, 457–472 (2015).
4. Adler, M. E. Signaling Breakthroughs of the Year. *Sci. Signal.* **10**, eaam5681 (2017).
5. Katsikis, P. D., Schoenberger, S. P. & Pulendran, B. Probing the 'labyrinth' linking the innate and adaptive immune systems. *Nat. Immunol.* **8**, 899–901 (2007).
6. Iwasaki, A. & Medzhitov, R. Toll-like receptor control of the adaptive immune responses. *Nat. Immunol.* **5**, 987–995 (2004).
7. Schimmelpfennig, C. H. *et al.* Ex Vivo Expanded Dendritic Cells Home to T-Cell Zones of Lymphoid Organs and Survive *in Vivo* after Allogeneic Bone Marrow Transplantation. *Am. J. Pathol.* **167**, 1321–1331 (2005).
8. Randolph, G. J., Angeli, V. & Swartz, M. A. Dendritic-cell trafficking to lymph nodes through lymphatic vessels. *Nat. Rev. Immunol.* **5**, 617–628 (2005).
9. Wu, W. *et al.* Structure-Activity Relationships in Toll-like Receptor-2 agonistic Diacylthioglycerol Lipopeptides. *J. Med. Chem.* **53**, 3198–3213 (2010).
10. Buwitt-Beckmann, U. *et al.* Lipopeptide structure determines TLR2 dependent cell activation level. *FEBS J.* **272**, 6354–6364 (2005).
11. Pawlak, J. *et al.* Bioorthogonal Deprotection on the Dendritic Cell Surface for Chemical Control of Antigen Cross-Presentation. *Angew. Chem. Int. Ed.* **54**, 5628–5631 (2015).
12. Parasar, B. & Chang, P. V. Chemical optogenetic modulation of inflammation and immunity. *Chem. Sci.* **8**, 1450–1453 (2017).
13. Liu, H., Kwong, B. & Irvine, D. J. Membrane Anchored Oligonucleotides for *in vivo* Tumor Cell Modification and Localized Cancer Immunotherapy. *Angew. Chem. Int. Ed.* **50**, 7052–7055 (2011).
14. Govan, J. M., Young, D. D., Lively, M. O. & Deiters, A. Optically Triggered Immune Response through Photocaged Oligonucleotides. *Tetrahedron Lett.* **56**, 3639–3642 (2015).
15. Parker, C. G., Domaal, R. A., Anderson, K. S. & Spiegel, D. A. An Antibody-Recruiting Small Molecule That Targets HIV gp120. *J. Am. Chem. Soc.* **131**, 16392–16394 (2009).
16. Kim, J. *et al.* Activation of Toll-Like Receptor 2 in Acne Triggers Inflammatory Cytokine Responses. *J. Immunol.* **169**, 1535–1541 (2002).
17. Mancini, R. J., Stutts, L., Moore, T. & Esser-Kahn, A. P. Controlling the Origins of Inflammation with a Photoactive Lipopeptide Immunopotentiator. *Angew. Chemie. Int. Ed.* **54**, 5962–5965 (2015).
18. Martín-Fontecha, A., Lanzavecchia, A. & Sallusto, F. Dendritic Cell Migration to Peripheral Lymph Nodes in Dendritic Cells. 31–49 (Springer Berlin Heidelberg, 2009).
19. Martín-Fontecha, A. *et al.* Regulation of Dendritic Cell Migration to the Draining Lymph Node. *J. Exp. Med.* **198**, 615–621 (2003).
20. Spohn, R. *et al.* Synthetic lipopeptide adjuvants and Toll-like receptor 2—structure—activity relationships. *Vaccine* **22**, 2494–2499 (2004).
21. Kang, J. Y. *et al.* Recognition of Lipopeptide Patterns by Toll-like Receptor 2-Toll-like Receptor 6 Heterodimer. *Immunity* **31**, 873–884 (2009).
22. Lee, H. W. *et al.* Tracking of dendritic cell migration into lymph nodes using molecular imaging with sodium iodide symporter and enhanced firefly luciferase genes. *Sci. Rep.* **5**, 9865 (2015).
23. Bertho, N. *et al.* Efficient migration of dendritic cells toward lymph node chemokines and induction of TH1 responses require maturation stimulus and apoptotic cell interaction. *Blood* **106**, 1734–1741 (2005).
24. Ritter, U. *et al.* Analysis of the CCR7 expression on murine bone marrow-derived and spleen dendritic cells. *J. Leukoc. Biol.* **76**, 472–476 (2004).
25. Noor, S. *et al.* CCR7-Dependent Immunity during Acute *Toxoplasma gondii* Infection. *Infect. Immun.* **78**, 2257–2263 (2010).
26. Clatworthy, M. R. *et al.* Immune complexes stimulate CCR7-dependent dendritic cell migration to lymph nodes. *Nat. Med.* **20**, 1458–1463 (2014).
27. Drew, E., Merzaban, J. S., Seo, W., Ziltener, H. J. & McNagny, K. M. CD34 and CD43 Inhibit Mast Cell Adhesion and Are Required for Optimal Mast Cell Reconstitution. *Immunity* **22**, 43–57 (2005).
28. Linterman, M. A. *et al.* CD28 expression is required after T cell priming for helper T cell responses and protective immunity to infection. *eLife* **3**, e03180 (2014).
29. Mempel, T. R., Henrickson, S. E. & von Andrian, U. H. T-cell priming by dendritic cells in lymph nodes occurs in three distinct phases. *Nature* **427**, 154–159 (2004).
30. Baltimore, D. Discovering NF- $\kappa$ B. *Cold Spring Harb. Perspect. Biol.* **1**, a000026 (2009).
31. Gerondakis, S. & Siebenlist, U. Roles of the NF- $\kappa$ B Pathway in Lymphocyte Development and Function. *Spring Harb. Perspect. Biol.* **2**, a000182 (2010).
32. Livak, K. & Schmittgen, T. Analysis of relative gene expression data using real-time quantitative PCR and the 2(-Delta Delta C(T)) Method. *Methods* **25**, 402–408 (2001).

## Acknowledgements

We would like to thank the Prescher Laboratory for help with IVIS imaging. The authors acknowledge the financial support provided by NIH (1U01A1124286-01 and 1DP2A112194-01), Prof. Esser-Kahn thanks the Pew Scholars Program, the Cottrell Scholars Program for generous support. This work was supported, in part, by a grant from the Alfred P. Sloan foundation.

## Author Contributions

K.R. designed and performed experiments, analyzed data, and wrote the manuscript. R.J.M. initially synthesized the photocaged agonist. B.M., T.K., and T.M. performed mouse experiments. A.P.E. supervised the project. All authors provided comments and contributions and have given approval to the final version of the manuscript.

## Additional Information

**Supplementary information** accompanies this paper at doi:10.1038/s41598-017-08520-x

**Competing Interests:** The authors declare that they have no competing interests.

**Publisher's note:** Springer Nature remains neutral with regard to jurisdictional claims in published maps and institutional affiliations.



**Open Access** This article is licensed under a Creative Commons Attribution 4.0 International License, which permits use, sharing, adaptation, distribution and reproduction in any medium or format, as long as you give appropriate credit to the original author(s) and the source, provide a link to the Creative Commons license, and indicate if changes were made. The images or other third party material in this article are included in the article's Creative Commons license, unless indicated otherwise in a credit line to the material. If material is not included in the article's Creative Commons license and your intended use is not permitted by statutory regulation or exceeds the permitted use, you will need to obtain permission directly from the copyright holder. To view a copy of this license, visit <http://creativecommons.org/licenses/by/4.0/>.

© The Author(s) 2017